25th ABCM International Congress of Mechanical Engineering
October 20-25, 2019, Uberlândia, MG, Brazil

COB-2019-1362
EVALUATION OF TURBULENT PROPERTIES IN AORTAS WITH ASCENDING AORTIC ANEURYSM

Gabriela de Castro Almeida
Angela O. Nieckele
Ivan Fernney Ibanez
Bruno Alvares de Azevedo
Pontifícia Universidade Católica do Rio de Janeiro, Department of Mechanical Engineering, 22451-900, Rio de Janeiro, RJ, Brazil
gabriela.castro@aluno.puc-rio.br, nieckele@puc-rio.br, ing.aguilar04@gmail.com, azevedo@puc-rio.br

Pedro Soares Teixeira
FIT Center – Clínica de Performance Humana, 24220-331, Niterói, RJ, Brazil
pedrosote@gmail.com

Ilan Gottlieb
Casa de Saúde São José, 22271-080, Rio de Janeiro, RJ, Brazil
ilangottlieb@gmail.com

Marcelo Machado Melo
Instituto Nacional de Cardiologia, 22240-006, Rio de Janeiro, RJ, Brazil
mmmelo@icloud.com

Abstract. *This research examines the flow within the aorta of two patients with aneurysm of the ascending aorta. For each patient, two tomography images that were performed at intervals of different years were obtained. By assessing the tomography images, it was observed that one of the patients presented a volumetric growth of the aneurysm and the other patient did not suffer alterations in relation to the size of the aneurysm. This study aims to assess the relationship between aneurysm growth or non-growth regarding to turbulence quantities such as turbulent kinetic energy and maximum turbulent shear stress. Three dimensional models were generated from computed tomography angiography and image segmentation of aortas. The flow was obtained with a commercial software, ANSYS Fluent v18.1. The turbulent flow was modeled with the two-equation* κ *-* ω *turbulence model. It was verified that the results of the turbulent kinetic energy and the maximum principal Reynolds shear stress are quite similar. The patient with aneurysm growth presents high values of turbulent quantities in the incoming jet and near to the posterior wall, while the patient without the aneurysm growth presents lower values. The identification of particularities of the flow related to ascending aortic aneurysms obtained with the present analysis provide additional information to help patient diagnosis by doctors and it might help future patients in their medical treatments.*

Keywords: *aneurysm, CFD, turbulence, hemodynamic*

1. INTRODUCTION

Arterial aneurysm is an excessive dilation of the normal diameter of an artery. It can occur at aorta, the principal artery in the human body. Ascending aortic aneurysm is usually asymptomatic, therefore, it is frequently identified accidentally during imaging exams of a patient with other clinical indications (Standring, 2015). The causes of the growth of this type of aneurysm are not known precisely. Its evolution occurs in a silent way, however, its complications, like rupture and dissection of the aorta, are catastrophic events (Elefteriades, *et al.*, 2015).

Weigang et al. (2008) discusses that patients with ascending aortic aneurysm present considerable differences in the aorta flow patterns when compared to the flow pattern of healthy individuals. Gülan et al. (2018) observed that counterclockwise helical flow patterns are developed from the ascending aorta and are extended towards the aortic arch in the healthy case. In the aneurysmal case, however, it was found that large rotational regions were formed during the systolic phase, which shows qualitative similarity with vortex ring formation, i.e., a central jet, surrounded by two large vortices. From a fluid mechanical point of view, a sudden increase in diameter leads to a separation of the boundary layer and a separation bubble, and hence it is likely that there is an analogy between the separation, the associated turbulence and pressure loss and aneurysm growth (Gülan et al., 2018).

According to Adrian (2007), the single hairpin eddy is a useful paradigm that explains many observations in wall

turbulence. It can provide a mechanism for creating high Reynolds shear stress at the wall, low-speed streaks, and for transporting vorticity of the mean shear at the wall away from the wall and for transforming it into more isotropically distributed small scale turbulent vorticity. Therefore, the presence of coherent structures inside the aorta can also be applied to explain the formation of high shear stress and pressure regions, that can induce aneurism dilatation.

The main goal of this study is to analyze using Computational Fluid Dynamics (CFD) the flow field, focusing in turbulence variables, as turbulent kinetic energy and maximum principal turbulent Reynolds stress, inside the aorta of patients with ascending aortic aneurysm. Results from two consecutive years were analyzed for two patients, aiming to identify different flow behavior associated with aneurysm growth. The first one presented a growth in the dilatation of the aneurysm, while second patient did not present a significant aneurysm growth.

2. METHODOLOGY

The computed tomography angiography (CTA) exams of two patients in a time span of different years were selected for analysis. This research was approved by the ethics committee of the National Institute of Cardiology, INC/MS. From a series of CTA slices, the DICOM (Digital Imaging and Communication in Medicine) images were transferred to the software Mimics (Materialise, Belgium) and an image segmentation was performed with the software FIJI (open source image processing software based on ImageJ), generating a three dimensional (3D) model.

To determine the flow field, a grid test was performed and a mesh with 4×10^5 nodes was created, where the difference of the pressure drop at the main area of interest (ascending aorta) was inferior to 0.3%, when the mesh size was doubled.

The focus of this study is to analyze turbulent variables distribution during ventricular systole, to access its influence on the flow and aorta´s surface. At the period of the ventricular systole, the aortic walls are distended, providing their maximum diameter, with small variation due the vascular complacency. Thus, the analysis is performed considering the maximum physiological flow rate, which can be twenty-five liters per minute, assuming steady state, which is a more critical situation.

As a first simplification, the aorta´s surface was considered rigid, due to its small complacency (Viscardi, et al., 2010; Faggiano, et al., 2013; Rinaudo & Pasta, 2014). The gravity effects were also neglected, since the pressure variations are dominant over the force of gravity. As reported by Stuart & Kenny (1980), the blood behaves like a Newtonian fluid when the deformation rate varies above 50 s^{-1} (Long et al., 2004, Crowley & Pizziconi, 2005). Consequently, the use of a Newtonian fluid is often justified on the grounds that blood hemolysis is a result of strong shear flows and turbulence, which are characterized by high shear rates (Deutsch et al., 2006), and can be found in patients with ascending aortic aneurysm (Simão et al., 2017). In addition, under normal conditions, the blood can be considered as an incompressible fluid (Feijó & Zouain, 1988).

The turbulence was modeled based on the Reynolds average approximation, with the two-equation κ–ω SST model (Menter, 1994). The turbulence model was selected by comparing the numerical predictions with experimental data obtained in a similar aorta (Azevedo et al., 2017; Celis Torres et al., 2017).

To determine the flow field, the time average conservation of mass and momentum were solved:

$$\frac{\partial u_i}{\partial x_i} = 0 \quad ; \tag{1}$$

$$\frac{\partial \rho u_j u_i}{\partial x_j} = -\frac{\partial \hat{p}}{\partial x_i} + \frac{\partial}{\partial x_j}\left\{ \left(\mu + \mu_t\right)\left[\frac{\partial u_i}{\partial x_j} + \frac{\partial u_j}{\partial x_i}\right]\right\} \tag{2}$$

where x_i represents coordinates axes, u_i the time average component of the velocity vector, ρ the density, μ the molecular viscosity, μ_t the turbulent viscosity and $\hat{p}$ is the modified pressure, which includes the turbulent dynamic pressure, dependent on the turbulent kinetic energy κ

$$\hat{p} = p + \tfrac{2}{3}\,\rho\,\kappa \tag{3}$$

$$\kappa = \tfrac{1}{2}\overline{u_i' u_i'} \tag{4}$$

The κ-ω SST turbulent eddy viscosity is based on a combination of the κ-ε and κ-ω turbulence models (Menter, 1994), and the turbulent viscosity model $\mu_t = \xi\,\rho\,\kappa/\omega$ is computed by employing a blending factor ξ, and ω is the turbulent density dissipation.

It was assumed that the inlet aortic valve was not deformed during the two years for the two patients, and the same uniform velocity normal to the inlet was imposed for both cases. It was assumed an inlet turbulent intensity of 5% (Celis et al., 2017; Salazar et al., 2008) and the length scale to estimate the inlet specific dissipation was defined equal to the inlet valve diameter. No slip condition was imposed at the aorta´s surface. The outflow flow rate distribution was defined based on average values in the human body (Alastruey et al., 2016). The outflow boundary condition at the descending aorta was 69.1%, at the three arteries at the top of the arch were defined as 19.3% (brachiocephalic artery), 5.2% (left

carotid artery), and 6.4% (left subclavian artery).

3. RESULTS AND DISCUSSION

The first parameter evaluated from both exams was the volume of the area of interest. During the time interval between exams, it was observed a volume growth of 10% for Patient 1 and inferior to 3% of volume growth for Patient 2, indicating an aneurysm growth for Patient 1 and no aneurysm growth for Patient 2.

The turbulent kinetic energy (TKE) κ represents the 'strength' of the turbulence in the flow, and caries the information of the three normal Reynolds stress tensor. Figures 1 and 2 show the turbulent kinetic energy distribution obtained from two exams gathered in different years, corresponding to Patient 1 and 2, respectively. At each figure a lateral view of the ascending aorta is shown in Figs. (a), as well as cross section planes transversal to the main flow (Figs. c). Figures (b) indicate the location of the transverse planes.

For Patient 1, Fig. 1, high turbulence values can be perceived near the entry and along the jet, until it reaches the anterior wall, where aorta dilatation occurs. In addition, the region with high turbulent kinetic energy levels increases from the first to the second year. On the other hand, while examining the turbulent kinetic distribution corresponding to Patient 2 in Fig. 2(i) and Fig. 2(ii), high κ values do not accompany the inlet jet. It can be seen low values of κ near to the anterior wall and high values close to the posterior part of the aorta. Further, lower κ values are observed for Patient 2 when compared with Patient 1, and different scales had to be employed.

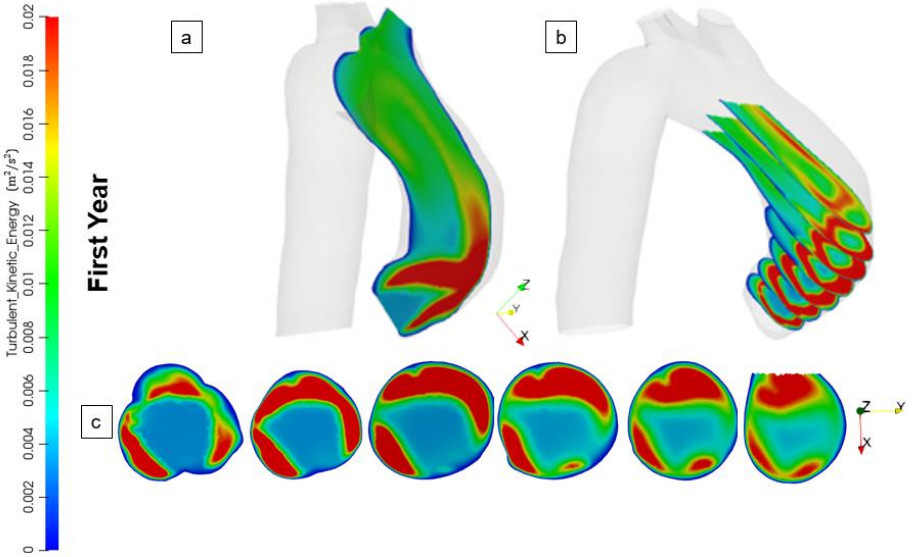

(i) Patient 1- 1st year

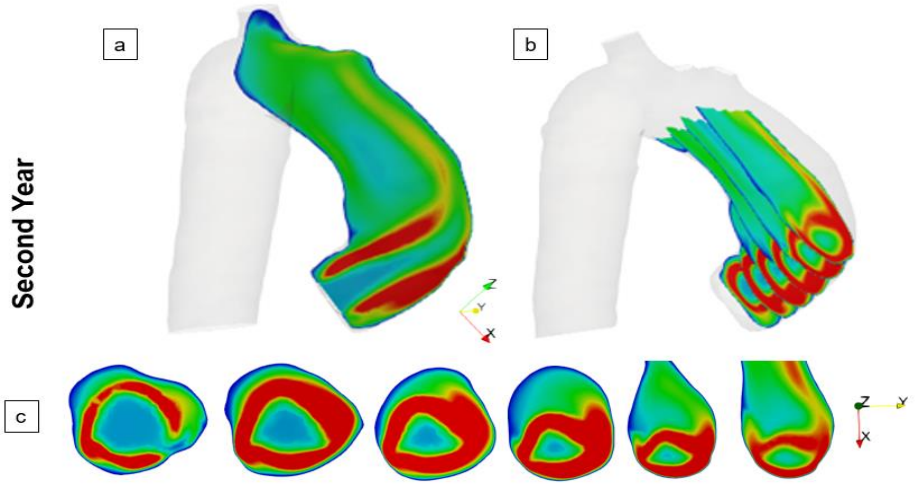

(ii) Patient 1 – 2nd year

Figure 1. Contours of turbulent kinetic energy of Patient 1. (a) Transverse planes. (b) Central plane. (c) Cross-sectional

individual plans

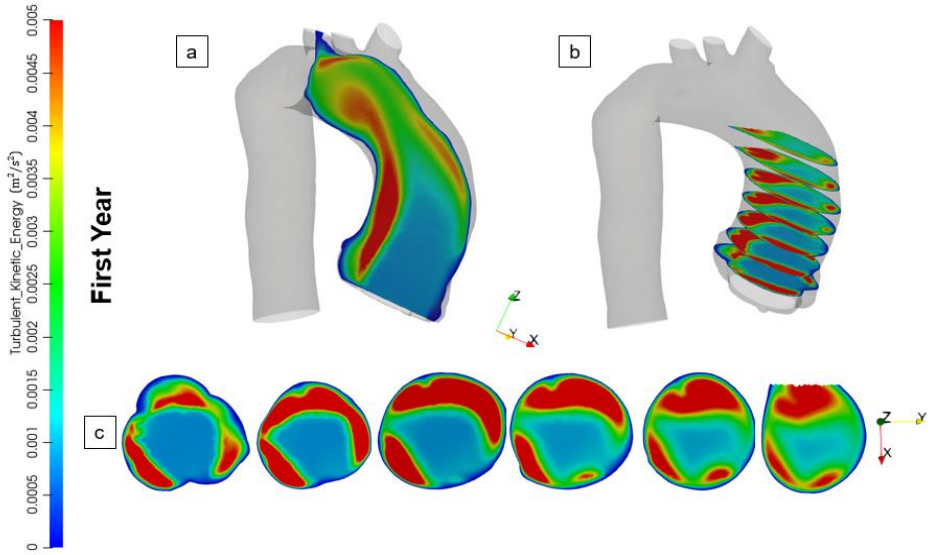

(i) Patient 2- 1st year

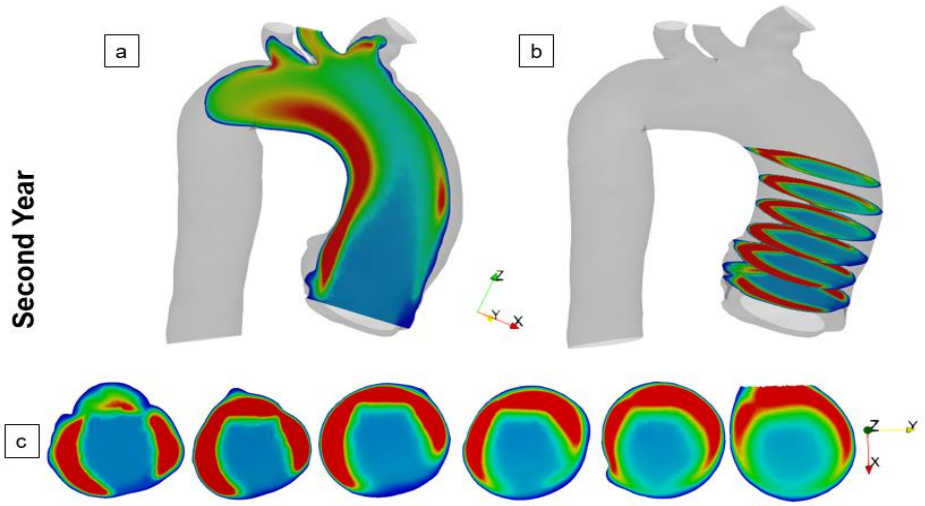

(ii) Patient 2 – 2nd year

Figure 2. Contours of turbulent kinetic energy of Patient 2. (a) Transverse planes. (b) Central plane. (c) Cross-sectional individual plans

Another very interesting turbulent variable is the maximum principal turbulent Reynolds stress acting on a surface element (de Tullio et al., 2009). High levels of stress on the blood cells are responsible for hemolysis and platelet activation (de Tullio et al., 2009). According to Sallam & Hwang (1984), the level responsible of incipient hemolysis ranges from 400 N/m² to 5 000 N/m². The investigation on the stress distribution (in particular, the turbulent Reynolds stress tensor distribution) is extremely important to evaluate its correlation to aneurysm growth.

The Reynolds stress tensor presents six components and it varies at each point of the domain. Nonetheless, when written in the principal coordinate system, it can be expressed in diagonal form, with only three principal normal stress σ_1, σ_2 and σ_3, ordered as $\sigma_1 \geq \sigma_2 \geq \sigma_3$. The identification of the principal normal stresses requires the solution of a third-order polynomial equation as

$$\sigma^3 - I_1\sigma^2 + I_2\sigma - I_3 = 0 \tag{5}$$

where I_1, I_2 and I_3 are the three stress invariants of the tensor

$$I_1 = \overline{u'u'} + \overline{v'v'} + \overline{w'w'} \tag{6}$$

$$I2 = \overline{u'u'}\ \overline{v'v'} + \overline{v'v'}\ \overline{w'w'} + \overline{u'u'}\ \overline{w'w'} - \overline{u'v'}^2 - \overline{v'w'}^2 - \overline{u'w'}^2 \tag{7}$$

and I_3 is the determinant of the Reynolds stress tensor and *u'*, *v'* and *w'* the fluctuations in velocity vector components in the three Cartesian directions.

The maximum turbulent shear stress acting on a surface element (Malvern, 1977), can be written as

$$TSS_{\max} = \frac{\sigma_1 - \sigma_3}{2} \tag{8}$$

where σ_1 and σ_3 are the maximum and minimum Reynolds stress in the principal axis.

In order to verify the existence of a correlation between the maximum principal turbulent shear stress distribution and aneurism growth, the TSS_{max} distributions for Patients 1 and 2 are shown in Figs. 3 and 4. The same type of layout for the images of the turbulent kinetic energy were employed here for presenting the TSS_{max} results.

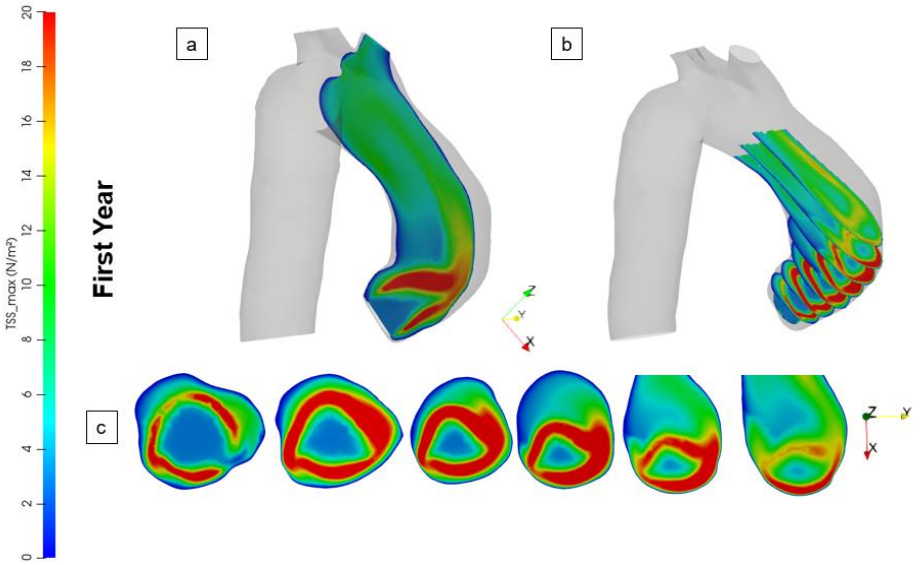

(i) Patient 1- 1st year

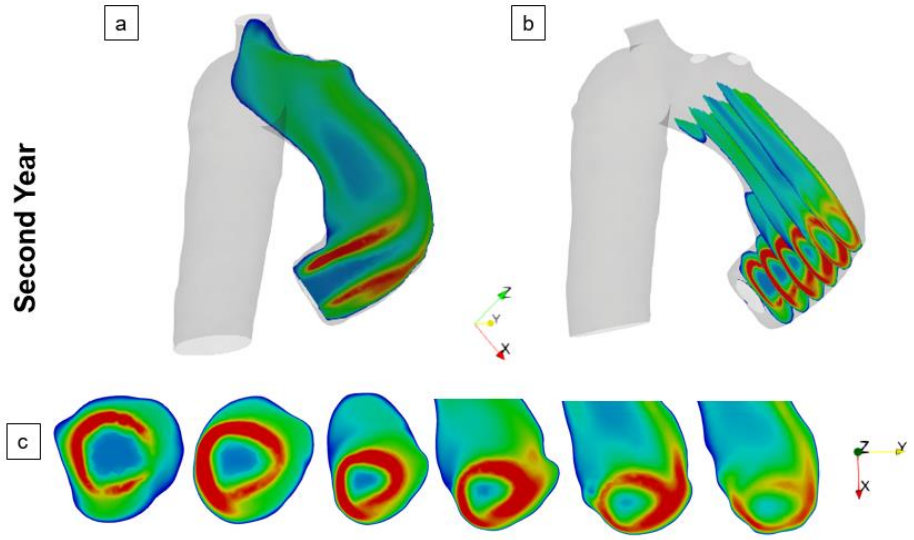

(ii) Patient 1 – 2nd year

Figure 3. Contours of maximum turbulent Reynolds shear stress of Patient 1. (a) Transverse planes. (b) Central plane.

(c) Cross-sectional individual plans

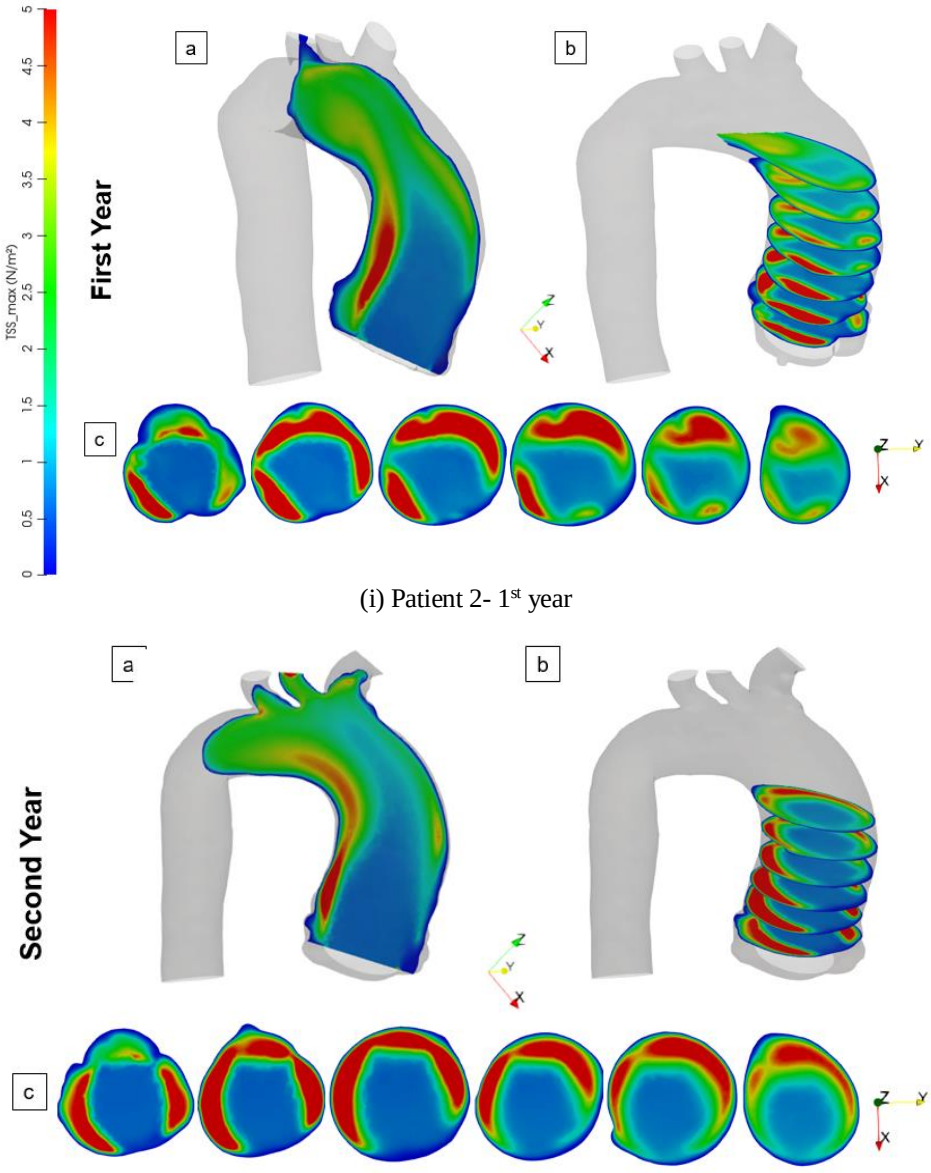

(i) Patient 2- 1st year

(ii) Patient 2 – 2nd year

Figure 4. Contours of maximum turbulent Reynolds shear stress of Patient 2. (a) Transverse planes. (b) Central plane. (c) Cross-sectional individual plans

Patient 1, Fig. 3(i) and Fig. 3(ii), shows higher values of TSS_{max} near to the anterior aorta wall, where the aneurysm growth is significant, while for Patient 2, Fig. 4(i) and Fig. 4(ii), the maximum value occurs in a region near to the posterior wall. High values of turbulent shear stress caused by the frictional force acting on the endothelial cell surface, according to Malek et al. (1999), may contribute to aneurysm's growth or rupture of the wall.

The distribution of the maximum turbulent Reynolds shear stress for Patients 1 and 2 are quite similar to the results presented of the turbulent kinetic energy. Les et al. (2010) established the relationship between the two variables. Turbulence kinetic energy and maximum turbulent Reynolds stresses both rely on a decomposition of the flow field into an average and fluctuating part, but the Reynolds stress computation is the ensemble of different components of the fluctuating velocity field $\sigma_{Re} = \rho\, \overline{u_i' u_j'}$. According to Les et al. (2010), when turbulence is high, it can be assumed that the fluctuating velocity fields are similar in magnitude ($|u_x'| \approx |u_y'| \approx |u_z'|$). In this way, the turbulent kinetic energy κ can relate to σ_{Re} as

$$\rho\,\kappa = \frac{1}{2}\rho\,\overline{u_i'^2} \approx \frac{3}{2}\left(\rho\overline{u_x'^2}\right) = \frac{3}{2}\sigma_{\mathrm{Re}} \tag{9}$$

Thus, the identification of regions with peaks of the turbulent kinetic energy can be related to the appearance of peaks of the maximum turbulent shear stress, and it was verified for both patients.

4. CONCLUSIONS

The flow field inside the ascending aorta of selected patients was numerically examined, by comparing turbulent variables. It was verified that the results of the turbulent kinetic energy and the maximum principal Reynolds shear stress are quite similar for both patients. However, high turbulent values can be perceived near to the entry and along the jet, until reaches the anterior wall, where aorta dilatation occurs for the patient who presented an aneurysm growth while for the patient that it did not grow, high turbulent values are seen at the posterior wall. The identification of the regions with high turbulent kinetic energy and the maximum principal Reynolds shear stress might aid the diagnosis of patients, indicating a higher probability of aneurism growth.

5. ACKNOWLEDGEMENT

This work was supported by the Cardiovascular Engineering Laboratory PUC-Rio. The authors also thank the Brazilian government agencies CNPq and CAPES for the continuous support.

6. REFERENCES

Adrian, R.J., 2007. “Hairpin vortex organization in wall turbulence”. *Physics of Fluids*, Vol. 19, No. 4, 041301.

Alastruey, J., Xiao, N., Fok, H., Schaeffter, T. & Figueroa, C. A., 2016. “On the impact of modelling assumptions in multi-*scale*, subject-specific models of aortic hemodynamics*”. J. R. Soc. Interface,13, 20160073.*

Azevedo, B. A., Camargo, G.C., dos Santos, J.R.L., Azevedo, L.F.A., Nieckele, A.O., Siqueira-Filho, A.G., Oliveira, G.M.M, 2017. “Influence of the tilt angle of Percutaneous Aortic Prosthesis on Velocity and Shear Stress Fields”. *Arq. Bras. Cardiol*. Vol.109, n.3.

Celis Torres, D., Ibañez, I., Nieckele, P. A., Nieckele, A. O., Azevedo, B. A., 2017, “Numerical investigation of hemodynamics patterns after Transcatheter Aortic Valve Replacement (TAVR)”. 2017. *Proceedings of the Congresso Brasileiro de Engenharia Mecânica (COBEM)*, Curitiba, COBEM-2017-0521.

Crowley, T.A., Pizziconi, V., 2005. “Isolation of plasma from whole blood using planar microfilters for a lab-on-a-chip applications”. *Lab on a Chip*, Vol. 5,No. 9, pp.922-929.

De Tullio, M.D., Cristallo, A.; Balaras, E.; Verzicco, R., 2009. “Direct numerical simulation of the pulsatile flow through anaortic bileaflet mechanical heart valve**”.** *J. Fluid Mech.*, Vol. 622, pp. 259-290.

Deutsch, S., Tarbell, J.M., Manning, K.B., Rosenberg, G., Fontaine, A.A., 2006. “Experimental fluid mechanics of pulsatile artificial blood pumps”. *Annual Review of Fluid Mechanics*, Vol.38, pp. 65-86.

Elefteriades J. A., Sang A., Kuzmik G., Hornick M., 2015. “Guilt by association: paradigm for detecting a silent killer (thoracic aortic aneurysm)”. *Open Heart*, 2:e000169.

Faggiano, E., Antiga, L., Puppini, G., Quarteroni, A., Luciani, G.B., Vergara, C., 2013. “Helicalflows and asymmetry of blood jet in dilated ascending aorta with normally functioning bicuspid valve”. *Biomechanics and Modeling in Mechanobiology,* Vol 12, No. 4, pp. 801-813.

Feijóo, R., & Zouain, N., 1988. “Formulations in rates and increments for elastic-plastic analysis”. *International Journal for numerical methods in engineering,* Vol. 26, No. 9, pp. 2031-2048.

Gülan, U., Calen, C., Duru, F., Holzner, M., 2018. “Blood flow patterns and pressure loss in the ascending aorta: A comparative study on physiological and aneurysmal conditions”. *Journal of Biomechanics*, Vol. 76, No.25, pp. 152–159.

Les, A.S., Shaddeb, S.C., Figueroa, C.A., Park, J.M.; Tedesco, M.M., Herfkens, R.J., Dalman, R.L.; Taylor, C.A., 2010. “Quantification of hemodynamics in abdominal aortic aneurysms during rest and exercise using magnetic resonance imaging and computational fluid dynamics”. *Annuals of Biomedical Engineering*, Vol. 38, No. 4, pp. 1288-1313.

Long, D.S., Smith, M.L., Pries, A.R., Ley, K., Damiano, E.R., 2004. “Microviscometryreveals reduced blood viscosity and altered shear rate and shear stress profiles in microvessels after hemodilution”. In *Proceedings of the National Academy of Sciences of the United States of America*, Vol. 101, No. 27, pp. 10060-10065.

Malek, A.M., Alper, S.L., Izumo, S., 1999. “Hemodynamic shear stress and its role in atherosclerosis”. *JAMA*, Vol. 282,

No. 21, pp. 2035-2042.

Malvern, L.E., 1977. “Introduction to the mechanics of a continuous medium”. Prentice Hall Inc.

Menter, F.R., 1994. “Two-equation eddy-viscosity turbulence models for engineering applications”. *AIAA Journal*, Vol. 32, No. 8, pp. 1598-1605.

Rinaudo, A., Pasta, S., 2014. "Regional variation of wall shear stress in ascending thoracic aortic aneurysms". *Proceedings of the Institution of Mechanical Engineers, Part H: Journal of Engineering in Medicine*, Vol. 228, No. 6, pp. 627-638.

Salazar, F.A., Rojas-Solórzano, L.R., Antaki, J.F., 2008. “Numerical study of turbulence models in the computation of blood flow in cannulas”. In *Proceedings of ASME Fluids Engineering Conference*, Jacksonville, FL, USA, pp. 999-1005.

Sallam, A.M., Hwang, N.H.C., 1984. “Human red blood cell hemolysis in a turbulent shear flow: contribution of reynolds shear stressess”. *Biorheology*, Vol. 21, No. 6, pp. 783-797.

Simão, M., Ferreira, J.M., Tomás, A.C., Fragata, J., Ramos, H.M., 2017. “Aorta ascending aneurysm analysis using CFD models towards possible anomalies”. *Fluids*, Vol. 31, No. 2, pp. 1-15.

Standring, S., 2016. *Gray's anatomy: the anatomical basis of clinical practice*. New York: Elsevier Limited, 41 Ed.

Stuart J.; Kenny, M.W., 1980. “Blood rheology”. *Journal of Clinical Pathology*, Vol. 33, No. 5, pp. 417-429.

Viscardi, F., Vergara, C., Antiga, L., Merelli, S., Veneziani,.A., Puppini, G., Faggian, G., Mazzucco, A., Luciani, GB., 2010. "Comparative finite element model analysis of ascending aortic flow in bicuspid and tricuspid aortic valve". *Artificial organs*, Vol. 34, No. 12, pp. 1114-1120.

Weigang, E., Kari, F.A., Beyersdorf, F., Luehr, M., Etz, C.D., Frydrychowicz, A., Harloff, A., Markl, M., 2008. “Flow-sensitive four-dimensional magnetic resonance imaging: flow patterns in ascending aortic aneurysms”. *European Journal of Cardio-thoracic Surgery*, Vol. 34, No. 1, pp. 11-16.

7. RESPONSIBILITY NOTICE

The authors are the only responsible for the printed material included in this paper.